ELSEVIER

Applied Surface Science 154–155 (2000) 577–586

applied surface science

www.elsevier.nl/locate/apsusc

Laser shaping of photonic materials: deep-ultraviolet and ultrafast lasers

P.R. Herman [a,*], R.S. Marjoribanks [b], A. Oettl [b], K. Chen [a], I. Konovalov [a], S. Ness [a]

[a] *Department of Electrical and Computer Engineering, University of Toronto, 10 King's College Rd., Toronto, ON, Canada M5S-3G4*
[b] *Department of Physics, University of Toronto, 60 St. George St., Toronto, ON, Canada M5S-1A7*

Received 1 June 1999; accepted 15 August 1999

Abstract

Optical materials are especially challenging to process with conventional lasers simply because of their high transparency. We are exploiting two extremes in laser technology — ultrafast lasers and very short wavelength F_2 lasers — to microsculpt surfaces and to control refractive index in transparent glasses. These lasers drive fundamentally different interactions, many-photon and 'big' photon, respectively, that offer distinct advantages and limitations for shaping photonic devices in fused silica. Comparisons of surface morphology, shock-induced microcracking, resolution, and photosensitivity responses are presented.

Keywords: Laser micromachining; Ablation; Photosensitivity; Ultrafast lasers; F_2-laser; Photonics

1. Introduction

Transparent glass materials provide the backbone of many of today's rapidly expanding photonics application areas, areas which serve such diverse fields as optical communications, electronics, sensor technologies, medicine, and materials processing. Electronic components are giving way to all-optical ones as new methods emerge to miniaturize and integrate optical components into compact functional systems offering high processing speeds. For optical communications, this means the development of planar lightwave circuits that combine directional couplers, add/drop filters, multiplexers, switches, wavelength converters, attenuators, and more onto a single 'chip'. This development is analogous to the first planarization and integration of transistor and other electronic components onto silicon four decades ago, constituting the birth of the exponentially growing electronic chip industry. Today's photonics industry holds equal promise, and is already tracking growth rates similar to the well-known Moore's law. In other optical application areas, fine feature-sizes are also required in diffractive optical elements, binary optics, miniature lens arrays, holographic optical storage, and masks for lithography.

As for the microelectronics industry, the future evolution of photonics will be dictated by the development of precise processing tools that can nanostructure optical materials. Because such devices are used to alter and control the pathway of light in optical systems, feature sizes only a small part of an

* Corresponding author. Tel.: +1-416-978-7722; fax: +1-416-971-3020.
E-mail address: hermanp@ecf.utoronto.ca (P.R. Herman).

0169-4332/00/$ - see front matter
PII: S0169-4332(99)00463-8

optical wavelength, i.e., ~100-nm for $\lambda/10$, are required for critical dimensions. One approach to processing includes the direct shaping of optical surface by micromachining or etching [1,2]. Alternatively, refractive index changes can be patterned internally in optical materials [3] as is currently done in fabricating fiber Bragg gratings with ultraviolet lasers [4]. For many of these applications, fused silica is the preferred material, providing high transparency, and stable properties over long lifetime and at high temperature. However, these ideal properties also present a challenge in material processing, especially on the scale of 100-nm feature size.

Laser material-processing is widely employed by the electronic industry today for trimming components, patterning the smallest features (~180 nm) in critical layers of silicon chips, etching structures, circuit repair, and metal-conductor deposition. Laser technology should be equally attractive as one means to process optical materials. However, because of the high transparency of fused silica, current industrial laser systems interact weakly with glass, and do not provide the control required in shaping optical devices. We are emphasizing two extremes in laser technology: ultrafast lasers that drive nonlinear material interactions with wide-bandgap glass, and the short-wavelength F_2 lasers that access defects or near-bandedge states to couple laser energy into the medium. These fundamentally different approaches offer distinct advantages and limitations for microsculpting surfaces and for writing refractive index structures in transparent glasses. Head-to-head comparison of these approaches is provided in this paper.

2. Laser–glass interactions

Fused silica has a ~9.3-eV bandgap energy, equivalent to 133-nm wavelength. For most industrially relevant lasers this means weak absorption and poor process control. Surface cracking and glass darkening are common features of such laser interactions. Fig. 1 shows a simple graph with pulse-duration and wavelength axes. The diagonal line depicts today's forefront in laser technology: the 157-nm F_2-laser at the top left representing extremely short wavelength sources on the nanosecond time scale, and the ultrafast lasers at the bottom right representing the shortest duration lasers available in the visible and near-infrared spectrum. Above this diagonal line are today's conventional lasers, which interact weakly and cannot process transparent glasses. Most promising are the forefront laser systems, F_2 and ultrafast. The 157-nm output of the F_2 laser, which strongly couples energy into glass via defects or near-bandedge states, provides one approach for micromachining glass [5,6] or driving refractive index change on nanosecond or longer time scales. A move towards longer wavelength sources requires nonlinear absorption processes — two-photon, three-photon, etc. — that is available with higher intensity [7–11]. However, shorter pulse duration is also necessary to deliver finite quantities of absorbed fluence into a controlled volume of material. The shape of the wavelength–pulse duration interface (in Fig. 1) for controlled processing of glass is poorly defined at present, depending on widely different laser-interaction physics and the criteria for high-quality laser processing.

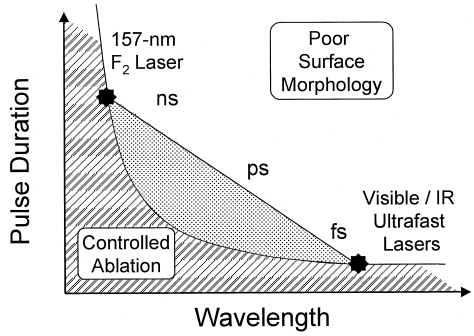

Fig. 1. Schema for micromachining of wide-bandgap transparent glasses, sketching pulse-duration and wavelength dependence. Conventional lasers (outside shaded regions) provide poor surface-morphology in micromachining glasses because of weak absorption. Glass processing requires forefront laser systems offering either short wavelength, e.g., F_2-laser, or intense ultrafast pulses (hatched area). In between, the boundary (grey shading) is not well-defined to date, and is likely a complex function of wavelength and pulse duration, and of the criteria for high-quality etching.

For long-pulse laser interactions with fused silica, high photon energy is essential for defining sub-micron features. Practical lasers are not yet available at the bandgap energy (9.3 eV). At 157 nm, fused silica is only weakly absorbing, $\alpha = 10\ \mathrm{cm}^{-1}$ [12], but F_2 lasers nevertheless provide sufficiently strong inter-

action that smooth etched surfaces can be precisely excised, free of microcracks and with little debris [1,5,6]. Vacuum–ultraviolet (VUV) lamp [13] and Raman laser [14,15] studies indicate an important role of Si–Si wrong bonds, which accumulate with exposure and may be responsible for the generation of copious densities of transient absorption species during a single laser pulse [14]. In our 157-nm ablation studies [6], etch rates followed a logarithmic fluence dependence as shown in Fig. 2. The inverse of the slope provides an effective single-photon absorption coefficient of $\alpha_{\text{eff}} = 170{,}000\ \text{cm}^{-1}$ — a 17,000-fold increase that attests to the importance of defect formation during such single-pulse interactions.

At a longer wavelength such as 193 nm, two-photon interactions are reported [16,17] to underlie compaction or refractive-index changes in fused silica. Longer wavelength lasers become amenable to glass processing when dopants such as germanium are added, for example, to define optical guiding regions in fibers or planar disks. Dopants lower the bandgap and provide copious new defect centres (e.g., Ge–O deficiency centres) that are central, for example, to strong photosensitivity responses and the commercial success of imprinting Bragg gratings inside fibers cores using ~ 240 nm [3,4]. Dopants also lower the ablation threshold. For 157-nm ablation, this threshold drops 70% to $\sim 0.38\ \text{J/cm}^2$ when 8% GeO_2 is doped into fused silica [1].

Extension to visible and longer-wavelength sources greatly diminishes the laser interaction. High-intensity laser sources become necessary to

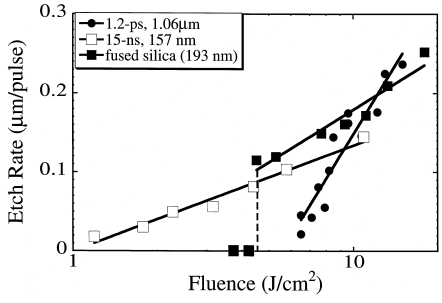

Fig. 2. Ablation etch rates of fused silica (Corning 7940) comparing 157-nm F_2 laser and 193-nm ArF laser with 1.2-ps 1.054-μm laser pulses. The solid lines are fitted by $D = (1/\alpha_{\text{eff}})\ln(F/F_{\text{th}})$. Values for α_{eff} and F_{th} [6,22] are given in Table 1.

micromachine surfaces cleanly by aggressively driving multiphoton, tunnel ionization, and electron-avalanche processes [7–11,18]. Absorbed fluence must also be controlled, and shorter pulses in the picosecond and femtosecond regime therefore become necessary. Much recent literature has been devoted to ultrafast laser damage and processing of transparent materials [7–11,18,19]. Attributes of ultrafast-laser micromachining include:

- nonlinear absorption mechanisms in transparent or wide-bandgap materials
- minimal collateral damage
- no plume development in short time scale; all laser energy reaches surface
- small interaction volume $< 1\ \mu\text{m}^3$
- flexibility processing by direct-write approach
- reproducible etch thresholds, for precision

Ultrafast lasers also offer the means to internally process transparent glass. Microexplosions [18] provide opportunities for 3-D optical storage while refractive index structures such as volume gratings [20] and waveguides [21] have been formed.

While ultrafast lasers offer exciting prospects for shaping photonic components, undesirable effects exist and processing windows are poorly defined [22]. Effects requiring more control include:

- incubation (defect generation) effects that change etching rates
- self focusing and clouding effects
- ‘gentle’ and ‘strong’ ablation phases developing with increasing number of pulses
- prepulse or pedestal effects
- poor morphology: periodic surface structures, melt, debris, surface swelling
- shock-induced microcracking

The development of viable laser processing must address these difficulties. A decade of research has been devoted to processing optical materials and fabricating photonic devices with lasers in our lab. The next section summarizes our findings by comparing ultrafast lasers with VUV lasers for micromachining fused silica.

3. VUV and ultrafast laser micromachining

The F_2 laser and 1-ps laser systems have been described elsewhere [6,23,24] and are only briefly described here. The home-built F_2 laser provided $\sim$35 mJ pulse energy at $\sim$5 Hz rate. The beam size was 3×12 mm^2 and the pulse duration was 15 ns. A narrow, 0.005 nm, spectrum provided large temporal coherence for interferometric applications. Ablation and photosensitivity studies were carried out using a

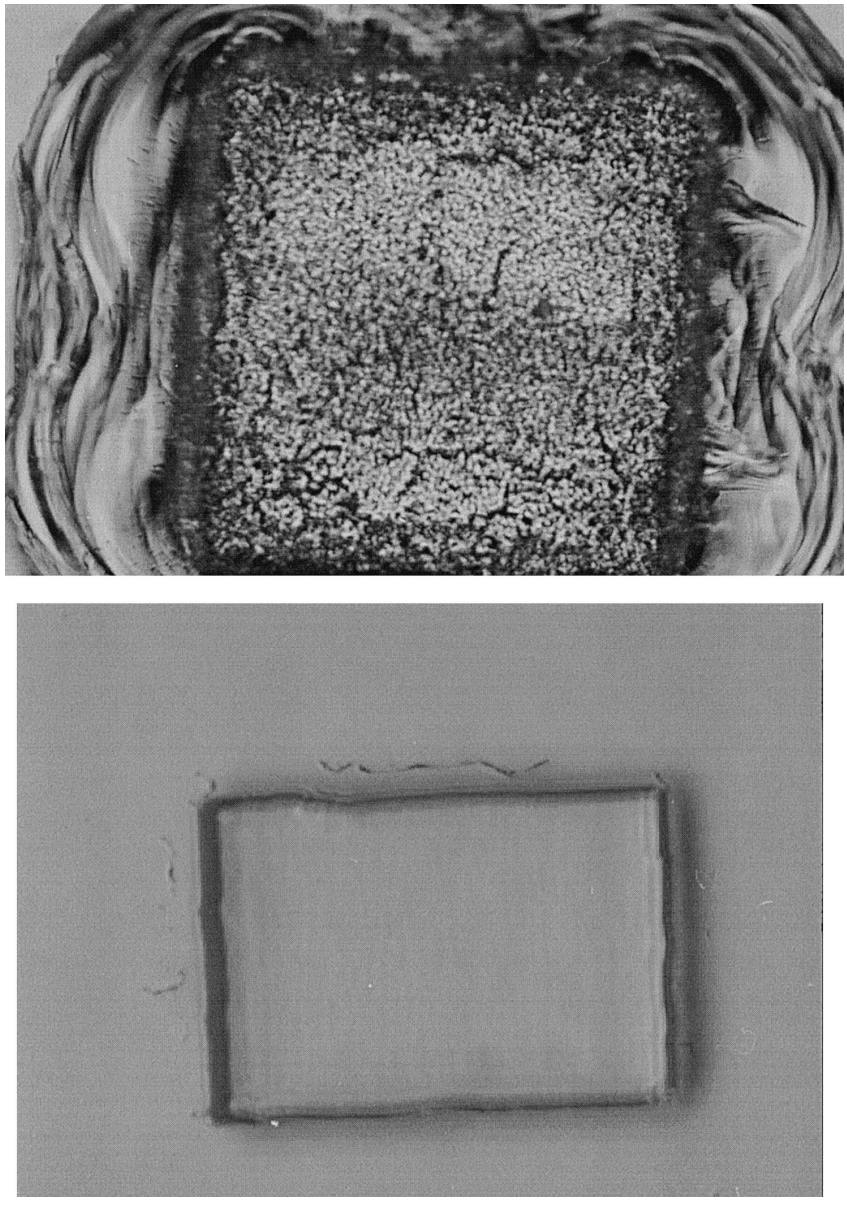

Fig. 3. Microscope photograph of optical waveguide (glass on silicon) etched by 193-nm (top) and 157-nm (bottom) lasers. At 193 nm, a single pulse at 3.6 J/cm^2 fluence mechanically ejected the whole 28-μm-thick layer of glass, leaving gross cracks in the glass and damage on the silicon underlayer. With 157-nm radiation, a smooth 6-μm-deep recess was precisely excised with 100 pulses at 3.0 J/cm^2 fluence. Excised areas are $\sim 225 \times 225$ μm^2 (top) and $\sim 180 \times 125$ μm^2 (bottom).

sealed vessel and beam tubes flushed with noble gas to avoid absorption by oxygen. A change of laser-gas mixture provided 193-nm radiation and 15-ns pulse duration.

The ultrafast laser consisted of a feedback-controlled Nd:glass oscillator (1.054 μm) operating at 1 Hz repetition rate. High-contrast single pulses of ~1 μJ energy could be selected from a flat-topped train of ~430 mode-locked pulses with 7.5-ns pulse-to-pulse separation; alternatively, the whole pulsetrain could be propagated to target. A 4-pass amplifier provided 13× gain for either the single-pulses or entire pulsetrains. Short focal-length aspherical lenses provided a variety of spot sizes from ~1.5 to 5 μm diameter (FWHM) on target surfaces.

3.1. VUV laser ablation

One promising platform for developing planar optical circuits is germanium-doped glass which offer low loss and efficient coupling into today's fiber-based optical communication systems. Fig. 3a shows the result of 193-nm ablation of such a waveplate grown on silicon substrate (PIRI SMPWL; 8 μm germanosilicate on 20 μm fused silica). The whole 28-μm-thick layer was ejected with a single pulse at 3.6 J/cm^2 fluence, leaving behind a damaged silicon surface and fractured glass edges. The gross mechanical ejection is presumably the result of laser heating at the glass–silicon interface. The glass is too transparent at 193 nm for delicate structuring of waveguide and similar components on such optical platforms. Fig. 3b shows the outcome using 100 pulses of 157-nm laser light at similar single-shot fluence. A smooth uniform excision of 6-μm depth was produced over a ~125×180 μm^2 area. A 60 nm/pulse etch rate attests to the excellent control of feature depth that is most promising for shaping photonic components. As a practical demonstration, Fig. 4 shows a smooth rib waveguide shaped on the same glass/silicon platform. The resulting rib waveguides are single mode at visible wavelengths and have a modest loss of ~3 dB/cm [1]. The results demonstrate that smooth optical-quality structures can be excised into doped glasses.

Fig. 2 shows the results of etch rate measured in fused silica for both 157- and 193-nm lasers. For 157-nm ablation, incubation effects were not noted, as etch depths proceed linearly with the number of laser pulses. (Incubation effects are noted at fluences below the 1.1 J/cm^2 ablation threshold. Glass compaction and increase in refractive index eventually give way to ablation when several hundred or thousand low-fluence laser pulses irradiate the surface.) Above the ablation threshold, etch depths closely follow a logarithmic fluence dependence with surface depth control of 20 nm at the lowest fluences. Atomic force micrographs (AFM) of etched surfaces

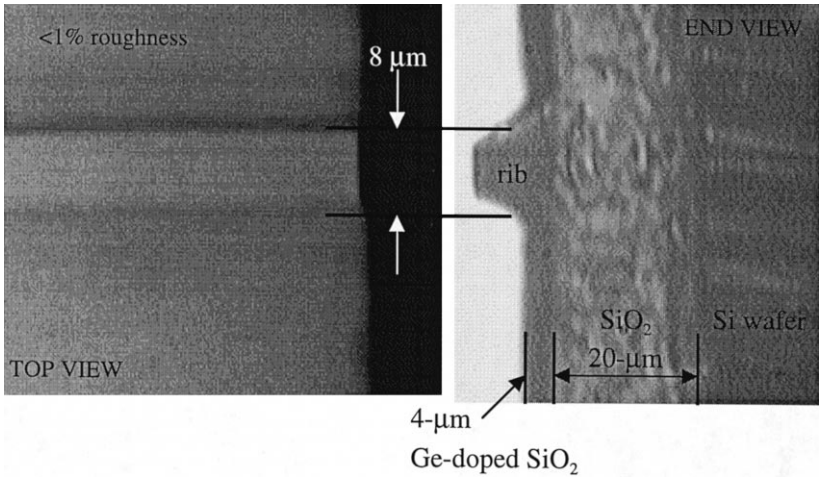

Fig. 4. Microscope photograph of top view (left) and end view (right) of a single-mode rib waveguide formed on a germanosilicate optical circuit by 157-nm laser ablation [1].

reveal a short-range periodic ($\Lambda \sim 5$ μm) surface roughness of ~ 6 nm rms amplitude as shown in Fig. 5. A longer-range surface roughness of ~ 15 nm rms was also noted over larger inspection areas (~ 60 μm $\times 60$ μm) and may be due to inhomogeneity in the laser beam. This latter surface roughness is of the order of 1% to 0.1% of the hole depth, and constitutes an exceptional smoothness that is only a fraction of an optical wavelength as required for shaping optical components.

The 193-nm etch rates in Fig. 2 were derived from 'incubated' surfaces. A prompt ablation threshold of ~ 4.5 J/cm^2 is noted below which ablation will not develop even after hundreds of laser exposures. Just above the prompt ablation threshold, surface swelling (~ 57 nm in 20 pulses) was observed before the development of a steady-state etching rate of ~ 120 nm/pulse. Surface morphology is much worse than for 157-nm ablation, and on occasion, surface cracks will form in certain grades of fused silica. The prompt ablation threshold is a signature of the 2-photon interactions underlying absorption at this wavelength. Only when larger fluences (~ 10 J/cm^2) are applied, does surface morphology improve somewhat and etching rates become more predictable. However, the 200-nm etch rate at such high fluence is too coarse for precise shaping of photonic components. To obtain better results at 193 nm, shorter pulses in the picosecond domain should be applied to drive stronger two-photon processes.

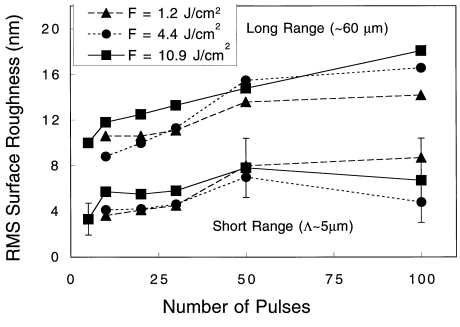

Fig. 5. Surface roughness (rms) of 157-nm ablated fused silica (Corning 7940) as a function of pulse number. AFM revealed both long- and short-range surface roughness which showed little dependence on either the laser fluence or the number of laser pulses. The short-range roughness is approximately periodic ($\Lambda \sim 5$ μm) [22].

3.2. Ultrafast laser ablation

We have previously reported results of 1.2-ps ablation of fused silica [22]. A 'gentle' ablation-processing window was identified in the 5.5–45 J/cm^2 fluence range where incubation effects were not observed over a small number of laser pulses. Etch rates for this 'gentle' ablation phase are plotted in Fig. 2. An AFM profile of a region etched by a single pulse at 38 J/cm^2 is shown in Fig. 6. Relatively smooth features of $\sim 10\%$ rms surface roughness is noted in this fluence window, with profiles which approximately follow the Gaussian intensity distribution. Single-pulse etch rates and threshold fluence (5.5 J/cm^2) were in general agreement with observations by other ultrafast laser studies [8,11]. The observed logarithmic fluence dependence on etch rate (Fig. 2) is surprising here, considering the nonlinear mechanisms that are understood to underlie interactions in transparent materials. Kautek et al. [25] have also reported a logarithmic fluence dependence for 150-fs to 3-ps ablation of borosilicate glasses. The data in Fig. 2 show that precise etch depth control of ~ 20 nm is also available with 1.2-ps pulses when near-threshold laser fluence is applied. This level of control is very similar to that provided by nanosecond-range pulses at 157 nm wavelength.

While these 1.2-ps observations appear promising for controllable etching of optical materials, detrimental effects are noted. Most significant is the development of shock-induced microcracks and shearing and flaking of surrounding surfaces followed a small number of moderate-intensity pulses. The threshold number, N_c, for crack development is fluence-dependent, following approximately $N = 1.7 + 80/F$, where F is the per-pulse fluence. To avoid gross cracking of surfaces, structures must be restricted to depths less than ~ 1 μm, still a reasonable stricture for several photonic-device fabrication applications. Varel et al. [26] also observed microcrack formation around deep (~ 1 mm) channels formed in fused silica by hundreds of 100-fs to 30-ps laser pulses. However, one favorable trend was a reduced microcrack formation with decreasing pulse duration. Shorter pulses also appear favorable, as noted by Kruger et al. [27], when using 20-fs pulses to improve the smoothness of holes in glass surfaces.

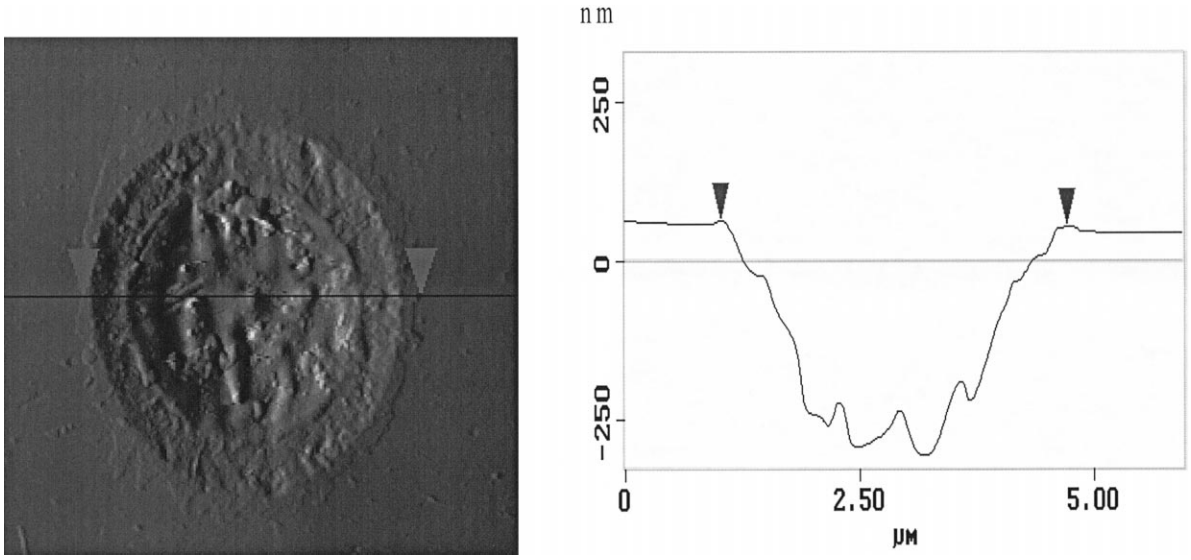

Fig. 6. AFM image (left) and depth profile (right) of a micro-holed excised in fused silica with a single 1.2-ps laser pulse of 1.054-μm wavelength and 38 J/cm^2 peak fluence. The 2-μm diameter (FWHM) hole has a ~10% rms surface roughness.

Current research in our laboratory [22] is showing much promise in eliminating microcrack formation altogether, by pulsetrain-burst machining. By applying the full oscillator pulse train (~430 pulses), local glass surfaces heat quickly because of the poor heat transport during the 7.5-ns time between pulses. An envelope of high-temperature glass localizes around the forming hole, improving the glass ductility, and thereby preventing microcrack formation at the hole edges. We are currently trying to identify the degree of depth-control that this approach will support.

In addition to microcracking, other undesirable ultrafast-processing effects include the occasional observation of slight surface swelling [22], and incubation effects that increase the etch rate with accumulated pulse number [28]. However, the present 1.2-ps results show that by restricting the laser parameters to a narrow fluence window and a small number of laser pulses, relatively smooth (~10%) surface structures can be ablated in transparent glasses with infrared picosecond laser pulses.

3.3. VUV and ultrafast comparison

Table 1 summarizes many of the ablation observations discussed above for fused silica. Of the VUV-nanosecond and 1.2-ps near-infrared lasers, the F_2

Table 1
Comparison of ultrafast and VUV laser micromachining of fused silica (Corning 7940)

Parameter	ArF laser (193 nm, 15 ns)	F_2-laser (157 nm, 15 ns)	Ultrafast Nd:glass (1.054 μm, 1.2 ps)
$1/\alpha_{eff}$ (nm)	96	59	250
prompt F_{th} (J/cm^2)	5.5	1.1	5.5
α_{eff} F_{th} (kJ/cm^3)	–	187	231
min. etch depth (nm)	125 nm	20 nm	20 nm
resolution	180 nm	120 nm	500 nm
surface roughness[a] (rms)	–	0.1–1%	10%
microcracks	occasional	no	yes
incubation	yes	~ no	yes
processing approach	mask projection	mask projection	scanning

[a] Relative to ablation depth.

laser provided the best surface morphology and control over etch depth without limitations from incubation effects, surface swelling or shock-induced microcracking. It is not surprising then that the F_2 laser provided the best values for ablation parameters. The penetration depth of $1/\alpha_{\text{eff}} = 59$ nm and the ablation threshold of $F_{\text{th}}, = 1.1$ J/cm^2 were the smallest of the three lasers tested. The short wavelength is also an advantage for shaping fine features; 120 nm surface relief gratings have been ablated on PMMA [29] while diffraction limits the tight focusing achievable with near-infrared laser light.

A survey of current laser applications in electronic component manufacturing shows that both scanning beam and mask projection approaches are widely used. This suggests that both F_2 and ultrafast lasers will eventually be applied to the nanofabrication of photonic components, the former serving mask-projection applications because of its large beam format and the latter supporting direct write or via etching because of its typically lower power and well-controlled Gaussian beam shape. While Table 1 represents the current state-of-the-art, better control over surface morphology and feature size is anticipated with the development of new lasers and systems for controlling pulse shape.

4. Controlling refractive index

When transparent glasses are irradiated at fluences below the ablation threshold, photochemical processes take place that permanently alter the refractive index of the medium. These 'radiation-damage' processes are related to the incubation effects described in the previous section, and are equally important in shaping useful photonic components. Theories of the mechanism behind this photosensitivity response fall into two camps: the colour centre model assumes that defect precursors within the glass network respond to sub-bandgap light and form new colour centres, changing the refractive index of the material through the Kramers–Kronig relationship; another popular theory emphasizes material compaction through radiation damage [4]. In either case, subtle laser interactions lead to useful and controllable amounts of refractive index change. These photosensitivity responses are widely employed today to print Bragg-gratings inside the core of optical fibers for application in optical telecommunication systems and sensors [4]. Our interest is in improving the photosensitivity responses of fused silica related materials by extending the laser source to the vacuum ultraviolet spectrum where new defect channels in glass may be accessed.

The photoinduced refractive-index changes in planar silica waveguides and bulk fused silica are reported for the first time at a record short wavelength of 157 nm. Unlike traditional ultraviolet sources, the 157 nm F_2-laser radiation was found to drive strong and rapid refractive-index changes without the need for enhancement techniques such as hydrogen loading [30], high germanium concentration [31], and ion implantation [32]. Such rapid responses are highly desired for fabricating miniature photonic components for optical communication networks.

The accumulated index change for single-mode slab waveguides of 3% $Ge0_2$–silica (PIRI Model SMPWL) is shown in Fig. 7 as a function of the product of the number of laser pulses, N, and the laser fluence. A uniform fluence exposure was used here. A maximum refractive-index changes of $\sim 9 \times 10^{-4}$ is noted after a total radiation dose of 4.5 kJ/cm^2. Bragg-grating structures ($\Lambda = 0.52$ μm) were also induced inside the wave-guiding layer using a phase mask and Sagnac interferometer. The 157-nm photosensitivity response is an order of magnitude above values found [33] with 193 nm or longer wavelength radiation, a record response with-

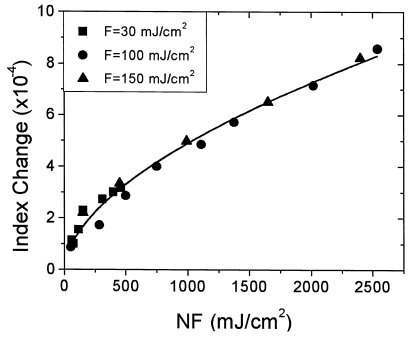

Fig. 7. Index-of-refraction changes in 157-nm irradiated germanosilicate as a function of the product of fluence and number of pulses. The data closely follow a universal compaction response, 9.67×10^{-6} $(NF)^{0.57}$ (F in J/cm^2), indicating a single-photon mechanism.

out the need for fiber sensitization techniques. An important extension of this work is the first demonstration of rapid index changes in ultraviolet-grade fused silica (Corning 7940). F_2-laser-induced index changes were as high as 10^{-4}, obtained at fluence responses exceeding previous reports [16,34] using 193 nm or longer wavelength lasers by an extraordinary three orders of magnitude. This value is large enough to imprint photonic devices inside pure fused silica.

The refractive index changes in both materials were found to follow a universal material compaction relationship of $\Delta n \sim (NF)^{0.5}$ where N is the number of pulses and F is the single-pulse fluence (see Fig. 7). Allan et al. [34] observed a nonlinear compaction response of $\sim (NF^2)^{0.53}$ for 193-nm laser irradiation of fused silica, providing evidence for a two-photon process. The linear fluence dependence at 157 nm points to a single-photon process associated with bandgap or near bandedge states such as oxygen deficiency centers. The mechanism may involve Si–O bond scission and the formation of the Si–Si wrong bond as noted in related VUV Raman laser studies of fused silica by Zhang et al. [15]. Fused silica samples were also examined by optical profilometry following 157-nm irradiation of 9000 pulses at 200 mJ/cm^2. The 1-mm-thick sample was compacted by ~ 200 nm, yielding a volume density change of $\delta\rho/\rho \sim 2 \times 10^{-4}$. Using the index-density change relationship, $\delta n = 0.4504\ \delta\rho/\rho$ [35], we infer an index change of 0.9×10^{-4}, in excellent agreement with our direct optical measurement of index change for the same net exposure. This observation therefore supports the compaction model for 157-nm refractive-index changes in glass.

The F_2 laser radiation can drive useful amounts of refractive index change in germanosilicate materials, and for the first time, in fused silica. The underlying mechanisms involve volume compaction of the material and the overall process is single photon unlike longer-wavelength interactions. Ultrafast lasers are equally interesting for writing large index changes in fused silica [18,35]. Gaeta [36] has reported refractive index changes as large as 10^{-4} when tightly focusing the 100-fs laser light inside borosilicate and fused silica glasses. Nonlinear interactions are a unique feature of ultrafast lasers that permits processing deeply inside the glass, a feature not possible with strongly absorbing ultraviolet lasers. This permits the formation of cylindrical waveguides [21,36] and offers excellent prospects for shaping novel 3-D photonic components in transparent glasses.

5. Conclusions

Research in our laboratories shows promising new directions for controlled processing of optically transparent materials with advanced laser systems. F_2 lasers and ultrafast lasers are key in driving strong absorption mechanisms in fused silica and related glasses that permit smooth nanosculpting of surfaces and the imprinting fine refractive-index structures. The laser approaches are distinctly different and will find photonic applications in separate niches that extend broadly in telecommunication, optical, electronic, sensor, and biomedical areas.

Acknowledgements

Funding from Photonics Research Ontario and the Natural Sciences and Engineering Research Council (Canada) are gratefully acknowledged.

References

[1] P.R. Herman, J. Yang, K. Kurosawa, T. Yamanishi, SPIE Proc. 2991 (1997) 170.
[2] K. Rubahn, J. Ihlemann, Appl. Surf. Sci. 127–129 (1998) 881.
[3] K.O. Hill, Y. Fujii, D.C. Johnson, B.S. Kawasaki, Appl. Phys. Lett. 32 (1978) 647.
[4] R. Kashyap, Fiber Bragg Gratings, Academic Press, New York, 1999.
[5] P.R. Herman, B. Chen, D.J. Moore, M. Canaga-Retnam, MRS Proc. 236 (1992) 53.
[6] P.R. Herman, K. Beckley, B. Jackson, K. Kurosawa, D. Moore, T. Yamanishi, J. Yang, SPIE Proc. 2992 (1997) 86.
[7] J. Ihlemann, Appl Surf. Sci. 54 (1992) 193.
[8] D. Du, X. Liu, G. Korn, J. Squier, G. Mourou, Appl. Phys. Lett. 64 (1994) 3071.
[9] W. Kautek, J. Kruger, SPIE Proc. 2207 (1994) 600.
[10] P.P. Pronko, S.K. Dutta, J. Squier, J.V. Rudd, D. Du, G. Mourou, Opt. Commun. 114 (1995) 106.
[11] B.C. Stuart, M.D. Feit, S. Herman, A.M. Rubenchick, B.W. Shore, M.D. Perry, J. Opt. Soc. Am. B 13 (1996) 459.
[12] D. Palik, Handbook of Optical Constants of Solids, Academic Press, New York, 1985.

[13] Y. Morimoto, T. Igarashi, T. Okanuma, J. Non-Cryst. Solids 179 (1994) 260.
[14] K. Sugioka, S. Wada, Y. Ohnuma, A. Nakamura, H. Tashiro, K. Toyoda, Appl. Surf. Sci. 96–86 (1996) 347.
[15] J. Zhang, K. Sugioka, S. Wasa, H. Tashiro, K. Toyoda, IEEE J. Sel. Top. Quantum Electron. 3 (1997) 1.
[16] M. Rothschild, D.J. Ehrlich, D.C. Shaver, Appl. Phys. Lett. 55 (1989) 1276.
[17] D.C. Allan, C. Smith, N.F. Borrelli, T.P. Seward III, Opt. Lett. 21 (1996) 960.
[18] C.B. Schaffer, A. Brodeur, N. Nishimura, E. Mazur, SPIE 3616 (1999) 143.
[19] Commercial and Biomedical Applications of Ultrafast Lasers, SPIE 3616 (1999).
[20] P.R. Herman, G. Goodno, X. Gu, J.B. Kalbfleisch, J. Long, M. Lukacs, R.S. Marjoribanks, R.J.D. Miller, M. Nantel, S. Ness, A. Oettl, SPIE 3618 (1999) 240.
[21] K.M. Davis, K. Miura, N. Sugimoto, K. Hirao, Opt. Lett. 21 (1996) 1729.
[22] P.R. Herman, A. Oettl, K. Chen, R.S. Marjoribanks, SPIE 3616 (1999) 148.
[23] P.C. Hill, P.R. Herman, R. Sia, J. Appl. Phys. 73 (1993) 5274.
[24] R.S. Marjoribanks, F.W. Budnik, L. Zhao, G. Kulcsar, M. Stanier, J. Mihaychuk, Opt. Lett. 18 (1993) 361.
[25] W. Kautek, J. Kruger, M. Lenzner, S. Sartania, C. Spielmann, F. Krausz, Appl. Phys. Lett. 69 (1996) 3146.
[26] H. Varel, D. Ashkenasi, A. Rosenfeld, M. Wahmer, E.E.B. Campbell, Appl. Phys. A 65 (1997) 367.
[27] J. Kruger, W. Kautek, M. Lenzner, S. Sartania, C. Spielmann, F. Krausz, Appl. Surf. Sci. 127–129 (1998) 892.
[28] A.C. Tam, J.L. Brand, D.C. Cheng, W. Zapka, Appl. Phys. Lett. 55 (1989) 2045.
[29] P.R. Herman, K. Beckley, R.A. Potyrailo, Vacuum–ultraviolet holographic gratings etched by a single F_2 laser pulse, CLEO, OSA Tech. Digest 8 (1994) 427.
[30] P.J. Lemaire, R.M. Atkins, V. Mizrahi, W.A. Reed, Electron. Lett. 29 (1993) 1191.
[31] E. Fertein, S. Legoubin, M. Douay, S. Canon, P. Bernage, P. Niay, F. Bayon, T. Georges, Electron. Lett. 20 (1991) 1838.
[32] J. Albert, B. Malo, K.O. Hill, D.C. Johnson, J.L. Brebner, R. Leonelli, Opt. Lett. 17 (1992) 1652.
[33] J. Albert, B. Malo, K.O. Hill, F. Bilodeau, D.C. Johnson, S. Theriault, Appl. Phys. Lett. 67 (1995) 3529.
[34] D.C. Allan, C. Smith, N.F. Borrelli, T.P. Seward III, Opt. Lett. 21 (1996) 960.
[35] N. Kitamura, Y. Toguchi, S. Funo, H. Yamashita, M. Kinoshita, J. Non-Cryst. Solids 159 (1993) 241.
[36] D. Homoelle, S. Wielandy, A.L. Gaeta, N.F. Borrelli, C. Smith, Opt. Lett. 24 (1999) 1311.